CARBOTHERMAL REDUCTION OF SILICA IN

HIGH TEMPERATURE MATERIALS

Nathan S. Jacobson

NASA Lewis Research Center
Cleveland, OH 44135

Abstract

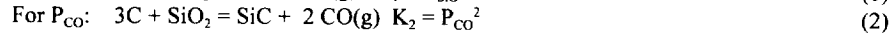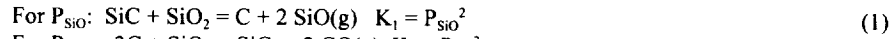The carbothermal reduction of SiO_2 to silicon occurs via a SiC intermediate. The SiO_2/SiC interaction is described with the Si-C-O stability diagram and superimposed SiO(g) and CO(g) isobars. Si-saturated SiC and SiO_2 generate much less total pressure of CO(g) and SiO(g) than C-saturated SiC and SiO_2. In many situations, a finite amount of carbon is in contact with SiO_2. If CO(g) is allowed to escape, the carbon activity will gradually decrease and the system will reach a point where P(CO) and P(SiO) are about equal. Experiments with C-saturated SiC and SiO_2 powders and the reduction of the oxide film on $MoSi_2$ powders confirm these predictions.
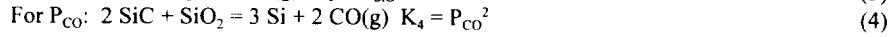
Introduction and Thermodynamic Considerations

The carbothermal reduction of SiO_2 is not only important in production of elemental silicon (1) but also such diverse areas as oxidation of SiC (2), protection of carbon/carbon by silicon carbide (3), and processing of $MoSi_2$ with carbon additions (4). In all cases, it is well established that silica initially forms SiC (5). Therefore, the key issue becomes the interaction of SiO_2 with SiC.

This system is best represented with the Si-C-O stability diagram (6), shown in Figure 1. This type of diagram indicates the stable phases for a given carbon and oxygen potential. At elevated temperatures, a gas phase composed of SiO and CO exists above these solids. The SiO and CO isobars are also shown in the diagram in Figure 1. As mentioned, the primary focus of this paper is on reactions at the SiO_2/SiC interface. Thus the relevant feature of the diagram becomes the line AB. The pressures of SiO(g) and CO(g) generated at this interface are given by the intersections of the SiO and CO isobars with this line. At point A, which is carbon-saturated SiC in contact with SiO_2, the SiO and CO pressures can also be calculated from:

For P_{SiO}: $\quad SiC + SiO_2 = C + 2\ SiO(g) \quad K_1 = P_{SiO}^2$ $\hfill (1)$

For P_{CO}: $\quad 3C + SiO_2 = SiC + 2\ CO(g) \quad K_2 = P_{CO}^2$ $\hfill (2)$

Similarly at point B, which is silicon-saturated SiC in contact with SiO_2, the SiO and CO pressures can be calculated from:

For P_{SiO}: $\quad Si + SiO_2 = 2\ SiO(g) \quad K_3 = P_{SiO}^2$ $\hfill (3)$

For P_{CO}: $\quad 2\ SiC + SiO_2 = 3\ Si + 2\ CO(g) \quad K_4 = P_{CO}^2$ $\hfill (4)$

Finally point C, which is between points A and B, is for the congruent reaction when SiC and SiO_2 react as follows:

$$SiC + 2\ SiO_2 = 3\ SiO(g) + CO(g) \quad K_5 = P_{SiO}^3\ P_{CO} \hfill (5)$$
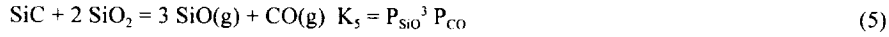
In this case there are three moles of SiO for every one mole of CO and the pressures are thus related by:

$$P_{SiO} = 3\ P_{CO} \hfill (6)$$

Thus the pressure of CO(g) in the congruent case can be calculated from:

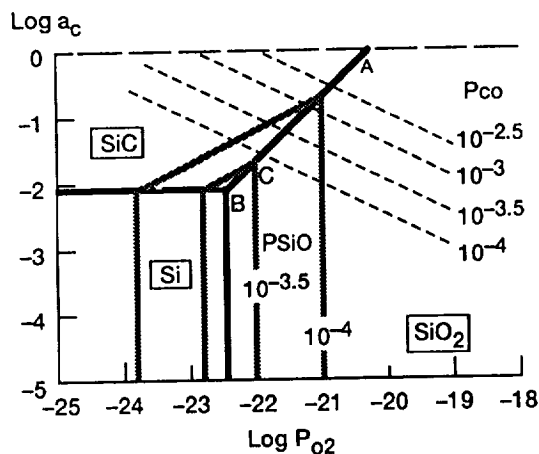$$K_5 = (3)^3\ P_{CO}^4 = 1/3\ P_{SiO}^4 \hfill (7)$$

Figure 1. Stability diagram for the Si-C-O system at 1500 K. The CO isobars are shown as dashed lines and the SiO isobars are shown as wide gray lines.

The stability diagram in Figure 1 is isothermal. The variation of total $P_{SiO} + P_{CO}$ pressure is shown in Figure 2 for carbon-saturated SiC in contact with SiO_2, silicon-saturated SiC in contact with SiO_2, and the congruent situation described above. Note that carbon-saturated SiC/SiO_2 gives a significantly higher pressure than silicon-saturated SiC/SiO_2. The congruent situation is between the two, but very close to the silicon saturated case.
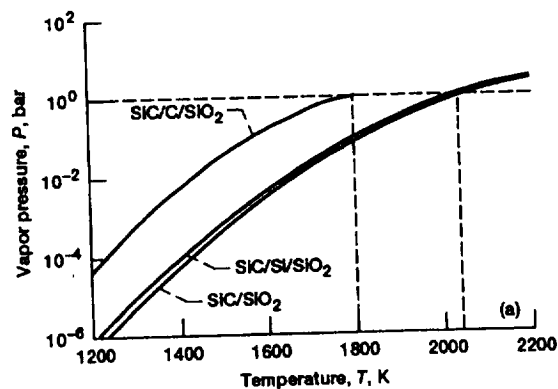

Figure 2. Total pressures of SiO(g) + CO(g) as a function of temperature for carbon-saturated SiC/SiO_2, silicon-saturated SiC/SiO_2, and the congruence point.

There is an immediate and important application of this difference in total gas pressures. Figure 3 is a schematic of the carbon/carbon protection system on the Space Shuttle. It consists of a

21

pack diffusion coating of SiC on the carbon/carbon, which is covered with a fluid SiO_2-based glass. In order to minimize reaction of SiC with the glass, the diffusion coating is intentionally made silicon-rich (3,7).

Glass Sealant

Silica

Silicon-saturated Silicon Carbide
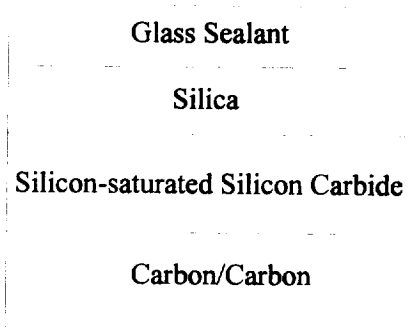
Carbon/Carbon

Figure 3. Schematic of coating system for carbon/carbon on wing leading edge and nose cone of space shuttle.

The stability diagram shown in Figure 1 can be applied to other situations as well. In many cases silica is in contact with a finite amount of carbon. Initially this situation is described by point A on Figure 1--SiC and a large amount of CO(g) forms. Figure 4 shows the ratio of CO to SiO along the SiC/SiO$_2$ coexistence line. Suppose we let the CO(g) escape--which is not strictly an equilibrium situation. The activity of carbon in the system decreases and we move down the SiC/SiO$_2$ co-existence line toward point B. This continues until P(CO) is close to P(SiO)--i.e. the activity of carbon in the system is no longer decreasing.
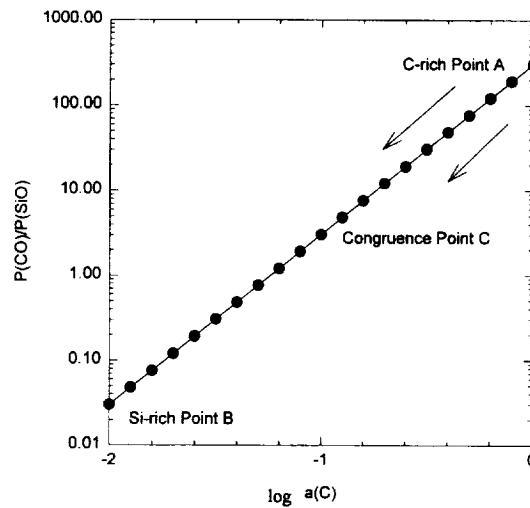

Figure 4. Variation of P(CO)/P(SiO) along line AB in Figure 1 at 1500 K.

22

Note that the system will not move all the way down to the Si region of Figure 1. It is well known that a mixture of carbon and silica will not produce silicon except at very high temperatures. A simple free energy minimum type calculation shows that pure Si is not thermochemically favored to form until about 2100 K (8,9).

The above predictions are illustrated with some Knudsen cell experiments on carbon-rich SiC and SiO_2. The predicitons are also applied to the carbothermal reduction of silica on $MoSi_2$ powders.

Experimental Procedure

The powders were heated in a Knudsen cell, which is a small container that allows solid and gas phases to equilibrate (10). A small orifice allows the vapor to be sampled. Generally, Knudsen cell measurements are taken only after equilibrium has been reached. However in this case the **approach** to equilibrium was particularly important.

A mixture of SiC with 2 w/o excess C and SiO_2 powders were reacted in a molybdenum Knudsen cell (11). A coating of molybdenum silicide, which was inert to reaction with this system, formed on the inner wall of the cell. Total vapor fluxes were monitored with a vacuum microbalance and the actual vapor composition was monitored with a mass spectrometer.

After these experiments, the microstructure of the powders was examined with a scanning electron microscope (SEM) and scanning Auger microscope (SAM).

Results and Discussion

Figure 5 shows this approach both in terms of total flux and P_{SiO} to P_{CO} ratio change. Initially the system exhibits a high total flux and a low P_{SiO} to P_{CO} ratio, indicating a high carbon activity. Then the flux decreases and the P_{SiO} to P_{CO} ratio increases, indicating a drop in carbon activity. Microstructural examination of the powders indicated that additional SiC formed during this period. Both the escape of CO(g) and formation of SiC effectively decreased the carbon activity. Equilibrium was attained with a P(SiO) to P(CO) ratio of about 2 to 1, which is close to that predicted.
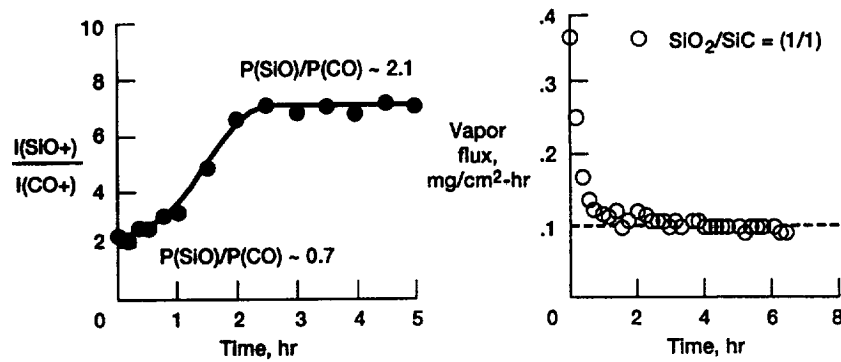
23

Figure 5. Ion intensity ratios of SiO(g) and CO(g) as a function of time, and total vapor flux as a function of time, for a mixture of carbon saturated SiC and SiO_2.

A further application the Si-C-O stability diagram is the addition of carbon to the $MoSi_2$ powders during processing (4). The carbon reduces the silica film on the particles and thus minimizes the presence of silica along the grain boundaries in the final product, leading to better mechanical properties. $MoSi_2$ powders with silica films were mixed with 2 w/o carbon and heated. Two mixtures were studied--one with 2.3 w/o oxygen on the $MoSi_2$ and one with 0.59 w/o oxygen on the $MoSi_2$. The reaction product composition and flux were analyzed at 1350 K using the Knudsen cell technique in the same way as the SiC/SiO_2 study.

First, consider the 2.3 w/o oxygen $MoSi_2$ powder mixture. The powders steadily lost weight for about 200 hrs. In this case, a large release of CO(g) was not recorded, rather an initial short (1 hr) burst of SiO(g) was recorded. The reasons for this are not clear--there may be excess Si in the $MoSi_2$. After about 2 hrs, the P(CO) to P(SiO) ratio became constant at about 1, consistent with the predictions and results for SiO_2/SiC system, discussed earlier. After this reaction, the powders were examined in a SAM and the results are shown in Figure 6(a) and 6(b). Note that a shell of SiC forms around the original $MoSi_2$ particle.
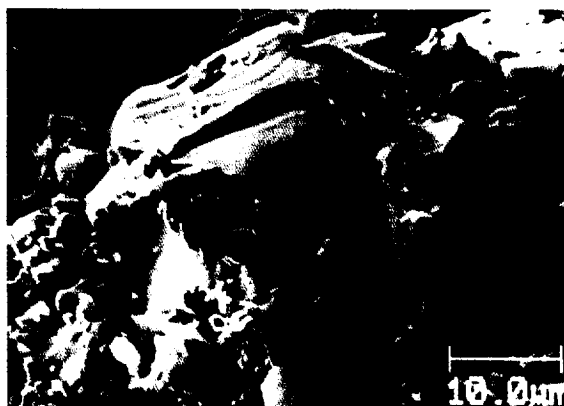
24

Figure 6(a). MoSi$_2$ + 2 w/o carbon after 4 hr reaction at 1350 K. Secondary electron image of a MoSi$_2$ particle covered by a SiC shell.
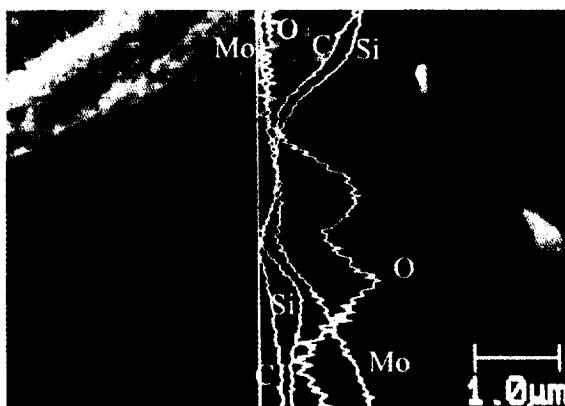

Figure 6(b). Auger line scans of particle shell in Figure 6(a).

These results are consistent with the SiC/SiO$_2$ results and the predictions from the Si-C-O stability diagram. Initially the system contains carbon and SiO$_2$. All of the carbon is consumed in reducing the SiO$_2$ to SiC. The carbon activity is reduced by the formation of SiC and the system comes to a steady state with P(CO) and P(SiO) about equal.

The 0.59 w/o oxygen MoSi$_2$ and carbon mixture showed somewhat different results. Again, a burst of SiO(g) was observed and then after about 2 hrs, the the P(CO) to P(SiO) ratio came to a constant value of about 20. In this case after all the SiO$_2$ is reduced to SiC, some free carbon

remains and the system is closer to point A on the stability diagram (Figure 1), as indicated by the $P(CO)$ to $P(SiO)$ ratio.

Summary and Conclusions

The Si-C-O system has been discussed in terms of the Si-C-O stability diagram. For the carbothermal reduction of silica, the SiC/SiO_2 coexistence line is the critical feature. Isobars of SiO and CO give the equilibrium gas pressure above these two phases at various positions on this SiO_2/SiC coexistence line. It is shown that silicon-saturated SiC in equilibrium with SiO_2 produces much lower pressures of SiO and CO than carbon saturated SiC in equilibrium with SiO_2. This is the reason the Space Shuttle's protective SiC coating on its carbon/carbon components is intentionally made silicon-rich. With a finite amount of carbon, it is predicted the carbon activity will decrease and the system will adjust to the point at which CO and SiO are in a ratio of about one. Experiments with SiC and SiO_2 powders confirm these predictions. The use of carbon to reduce the oxide film in $MoSi_2$ powders also gives results consistent with these predictions.

Acknowledgements

References

1. T. Rosenqvist, Principles of Extractive Metallurgy, 2nd Edition, McGraw Hill, New York, NY, 1983, ppp. 377-380.

2. N. S. Jacobson, "Corrosion of Silicon-Based Ceramics in Combustion Environments," J. Am. Ceram. Soc. 76 (1) (1993), 3-28.

3. R. A. Rapp and G. R. St. Pierre, "New Options for Protection of Carbon/Carbon Composites" (Report AFWAL-TR-87-4142, R. J. Kearns and L. S. Thiebert, eds., Wright Patterson AFB, p. 27)

4. N. S. Jacobson, K. N. Lee, S. A. Maloy, and A. H. Heuer, "Chemical Reactions in the Processing of $MoSi_2$ + Carbon Compacts", J. Am. Ceram. Soc. 76 (8) (1993), 2005-2009.

5. D. H. Filsinger and D. B. Bourrie, "Silica to Silicon: Key Carbothermic Reactions and Kinetics," J. Am. Ceram. Soc. 73 (6) 1726-1732 (1990).

6. D. R. Gaskell, "Phase Equilibria in Si-C-O Ceramic Matrix Composites," CIAC Newsletter, US Department of Defense Information Analysis Center, Perdue University, 1 (3) (1991).

7. N. S. Jacobson and R. A. Rapp, "Thermochemical Degradation Mechanisms for the RCC Panels on the Space Shuttle," (NASA Technical Memorandum, in press).

8. N. S. Jacobson and E. J. Opila, "Thermodynamics of the Si-C-O System," Met. Trans. 24A (1993), 1212-1214.

9. T. M. Besmann, "SOLGASMIX-PV, A Computer Program to Calculate Equilibrium Relationships in Complex Systems," ORNL Report TM-5775, Oak Ridge, TN, 1977.

10. J. L. Margrave (ed.), The Characterization of High Temperature Vapors (Wiley, New York, NY, 1967).

11. N.. S. Jacobson, K. N. Lee, and D. S. Fox,"Reactions of Silicon Carbide and Silicon (IV) Oxide at Elevated Temperatures," J. Am. Ceram. Soc. 75 (6) (1992) 1603-1611.